

Toward Generalist Semi-supervised Regression via Decoupled Representation Distillation

Ye Su^{1*}, Hezhe Qiao^{2*}, Wei Huang³, Lin Chen^{1†}

¹Chongqing Institute of Green and Intelligent Technology, Chinese Academy of Sciences

²Singapore Management University

³Beijing University of Posts and Telecommunications

suye@cigit.ac.cn, hezheqiao.2022@phdcs.smu.edu.sg, huangwei@bupt.edu.cn, chenlin@cigit.ac.cn

Abstract

Semi-supervised regression (SSR), which aims to predict continuous scores of samples while reducing reliance on a large amount of labeled data, has recently received considerable attention across various applications, including computer vision, natural language processing, and audio and medical analysis. Existing semi-supervised methods typically apply consistency regularization on the general regression task by generating pseudo-labels. However, these methods heavily rely on the quality of pseudo-labels, and direct regression fails to learn the label distribution and can easily lead to overfitting. To address these challenges, we introduce an end-to-end Decoupled Representation distillation framework (**DRILL**) which is specially designed for the semi-supervised regression task where we transform the general regression task into a Discrete Distribution Estimation (DDE) task over multiple buckets to better capture the underlying label distribution and mitigate the risk of overfitting associated with direct regression. Then we employ the Decoupled Distribution Alignment (DDA) to align the target bucket and non-target bucket between teacher and student on the distribution of buckets, encouraging the student to learn more robust and generalized knowledge from the teacher. Extensive experiments conducted on datasets from diverse domains—including audio, text, image, and medical data—demonstrate that the proposed DRILL has strong generalization and outperforms the state-of-the-art competing methods.

Introduction

Semi-supervised regression (SSR) aims to rank or predict sample values using deep learning methods while reducing reliance on a large amount of labeled data. It has been widely applied in various scenarios, including age estimation, clinical score prediction, and audio-based assessments. With the rapid advancement of deep learning in recent years, regression tasks using deep learning models across various domains have attracted significant attention (Yang et al. 2024; Van Engelen and Hoos 2020). Some approaches directly employ models such as CNNs for images and RNNs for time series, optimizing them with loss functions like MSE or MAE on the available labeled data (Mohammadi Foumani et al. 2024; Yang et al. 2022), see Fig. 1 (a). However, this straightforward application often risks overfitting, see Fig. 1 (b), especially in scenarios with limited labeled samples, as

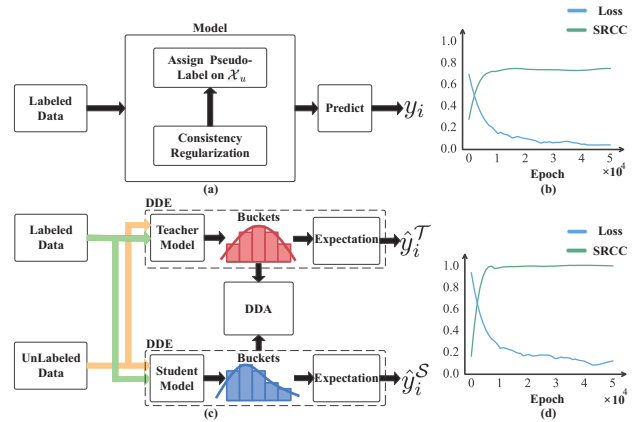


Figure 1: (a) The framework of existing SSR methods, which typically directly predict the score using MAE is referred to as Direct Regression (DR) methods. (c) The framework DRILL establishes an end-to-end decoupled representation distillation framework. (b) and (d) are the training loss (MAE) and test SRCC curves for DR and DRILL on the UTKFace dataset (Zhang, Song, and Qi 2017). DR achieves a very low training loss, but its lower SRCC indicates the risk of overfitting. In contrast, DRILL maintains a high SRCC as training converges, demonstrating its better generalization.

the performance of deep learning models heavily relies on the availability of labeled data. In real-world applications, obtaining a large amount of labeled data across diverse domains remains a persistent challenge. (Gui et al. 2024)

Therefore, several methods that assign the pseudo-labels on the unlabeled samples have been proposed to address this issue (Zhang et al. 2025; Zheng et al. 2025; Min, Bai, and Li 2024). Pseudo-labels are typically generated by training on the available labeled samples, and consistency regularization is often used to assist the optimization process. While pseudo-labeling helps mitigate the challenge of limited labeled data, overfitting may also occur, as incorrect labels are treated as true labels during training, the model is likely to overfit to the wrong annotations. The effectiveness of these approaches heavily relies on the quality of the pseudo-labels,

*Equal contribution

and assessing the reliability of the generated pseudo-labels remains a challenging task.

To address these challenges, we introduce an end-to-end decouple distillation framework (DRILL), which is specially designed for SSR, see Fig. 1 (c). DRILL is implemented through Discrete Distribution Estimation (DDE), which transforms the regression task into a distribution estimation problem. In this approach, the continuous ground truth values are divided into several buckets, and the model predicts a probability distribution over these buckets. By dividing continuous labels into discrete levels, the model can capture the inherent structure of the labels, enabling it to model the ordinal and interval relationships among them. This approach also effectively mitigates the risk of overfitting, as it offers a smoother learning objective and richer label distribution than direct numerical regression, especially when the training data is limited (see Fig. 1 (d)).

To further enhance generalization, we introduce a novel decoupling distribution alignment (DDA) approach, where we decouple the distribution into two parts for alignment, rather than aligning the distribution directly. The discrete distribution is the probability of the score being located in this bucket, and the final score can be estimated by the expectation, making the student learn more robust and more generalizable knowledge representation provided by the teacher. Although there are some attempts by applying the decouple distillation on the classification task (Zhao et al. 2022; Li, Wang, and Cui 2023; Feng et al. 2024). There is no work on semi-supervised regression. And the main difference here is that we aim to leverage the decoupled distribution alignment to highlight the target buckets and non-target buckets during the distillation, and the targets are recognized by the ground truth and generated pseudo labels, which help extract more fine-grained features, thereby avoiding overfitting and instability that may arise from directly fitting noisy or complex ground truth. Through distillation, we leverage the distribution over buckets for learning, avoiding sole reliance on pseudo labels and reducing the negative impact of incorrect pseudo labels on the model. In summary, this work makes the following main contributions.

- We for the first time built an end-to-end decouple distillation framework, DRILL, for semi-supervised regression, where we transform the direct regression into discrete distribution estimation (DDE) to mitigate the overfitting issue commonly encountered in direct regression.
- We further introduce a novel alignment method, decouple distribution alignment (DDA), which enables the student model to identify important buckets and mitigate the negative impact of noise. This facilitates the learning of richer and more accurate knowledge, thereby enhancing the generalization capability of the SSR task.
- Extensive experiments were conducted on the datasets from various domains, including audio, text, image, and medical data. The experimental results demonstrate that DRILL outperforms the state-of-the-art semi-supervised regression methods.

Related Works

Semi-supervised Learning

Semi-supervised Classification. Semi-supervised classification aims to improve classification performance by leveraging a small amount of labeled data along with a large amount of unlabeled data by generating the corresponding pseudo labels. The pseudo-label-based methods typically depend on the smoothness assumption that neighboring data points in the feature space tend to exhibit similar labels (Yang et al. 2022; Mey and Loog 2023; Berthelot et al. 2019; Sohn et al. 2020). The pesudo-label generation approach can effectively enhance the dataset and help the model learn fine-grained boundaries (Lee et al. 2013). As an effective way to refine the knowledge from existing methods, knowledge distillation is also used for pseudo generation, for example, Xie *et al.* present a pseudo-labeling approach based on knowledge distillation, using diverse student training techniques. This involves initially training a teacher model on labeled images to generate pseudo-labels for unlabeled examples (Xie et al. 2020b). Although some knowledge distillation methods have been applied to semi-supervised classification, their full potential has not been explored in the SSR task.

Semi-supervised Regression SSR refers to predicting continuous real-valued outputs rather than discrete class labels using a dataset that contains only a small subset of labeled instances. The semi-supervised regression methods can be roughly categorized into pseudo-label-based methods, consistency regularization, and surrogate task-based methods. Jo *et al.* (Jo, Kahng, and Kim 2024) propose an SSR framework that uses uncertainty estimation to guide pseudo-labeling, alongside a pseudo-label calibration approach that enhances pseudo-label quality by propagating information from labeled to unlabeled samples. Semi-supervised deep kernel learning (Jean, Xie, and Ermon 2018) minimizes predictive variance on unlabeled data through consistency regularization, leveraging the robust uncertainty quantification provided by Gaussian processes. Some surrogate task-based methods exploit the ranking information among samples as auxiliary for regression (Qiao, Chen, and Zhu 2022; Huang, Fu, and Tsao 2024). For example, Rankup (Huang, Fu, and Tsao 2024) constructs pairwise ranking labels from continuous targets and applies standard semi-supervised classification techniques with an auxiliary ranking classifier. Although these methods have achieved remarkable success in SSR, most of them directly predict a single continuous value, which makes them sensitive to noise and prone to overfitting. Therefore, instead of operating directly on the regression output, we transform the SSR to a discrete distribution estimation to mitigate the risk of overfitting, thereby leading to better performance.

Distribution Alignment in Distillation

Distribution alignment is a strategy used during student model training to match not only the outputs of the teacher model but also its underlying distributions. Existing approaches can be roughly categorized into logit-level alignment and feature-level alignment. Logit-level alignment

aims to align the output distribution (e.g., softmax probabilities) of the teacher and student (Hinton, Vinyals, and Dean 2015; Zhao et al. 2022). For example, the multi-level logit distillation method (Jin, Wang, and Lin 2023) employs multi-level prediction alignment to facilitate instance prediction learning in the student model. Curriculum temperature (Li et al. 2023) introduces temperature scheduling for dynamically adjusting softening intensity across training phases, which smooths gradient flow. The feature-level distribution alignment matches the representation, which is often done by maximum mean discrepancy, contrastive, and correlation-based loss (Gou et al. 2021; Chen et al. 2021). Notable advancements in feature-level distillation encompass DiffKD (Huang et al. 2023), training diffusion denoisers with teacher features to enforce attention map congruence in critical regions; WCoRD (Chen et al. 2021), constructing global-local hybrid contrastive objectives with Wasserstein dual loss to align deep geometric structures. These alignment approaches have demonstrated effectiveness in knowledge transfer. However, they struggle to capture fine-grained information, resulting in limited generalization. To address this, instead of aligning representations directly as in prior work, we propose DDA, which leverages the decouple representation distillation to align the distributions over buckets, enabling the student to learn richer and more generalized knowledge.

Methodology

Notations. We assume the data set \mathcal{X} consists of n labeled samples $\mathcal{X}_l = \{(x_i, y_i)\}_{i=1}^n$ and m unlabeled samples $\mathcal{X}_u = \{(x_i)\}_{i=m}^{n+m}$, with instance $x \in \mathbb{R}$ for image, text audio or tabular medical data. $\mathcal{Y} = \{y_i\}$ denotes the set of ground truth labels, where each label y_i is a continuous value in \mathbb{R} .

Problem Statement. Deep semi-supervised regression can be reformulated as given the training set \mathcal{X}_T and $\mathcal{X}_T = \mathcal{X}_l$, we aim to train a mapping function $f : \mathcal{X}_u \mapsto \mathcal{Y}$ which maps each input $x_i \in \mathcal{X}_u$ to a continuous scalar $y_i \in \mathbb{R}$. Some self-supervised methods extract features by capturing relationships between samples, and thus often include unlabeled data as input. Therefore, in this case, the \mathcal{X}_T consists of \mathcal{X}_l and \mathcal{X}_u .

The Overview of DRILL

As shown in Fig. 2, the proposed DRILL predicts scores by establishing a decoupled representation distillation framework, where the ground truth is transformed into a distribution over several buckets by DDE, effectively converting the regression task into a discrete distribution estimation problem for both teacher and student models. We then apply DDA over buckets to enable the student model to learn fine-grained and more generalized knowledge.

This distillation process is particularly effective for SSR task due to two key factors: (1) we reformulate the direct regression task as a discrete distribution estimation problem, which effectively mitigates the risk of overfitting of direct regression especially in the scenario that labeled samples are limited; and (2) we introduce a novel decoupled distribution alignment strategy for representation distillation over

the buckets, enabling the model to capture fine-grained features more effectively than conventional alignment methods. Finally, the model is jointly trained by combining the loss functions of the student and teacher, augmented with the proposed decoupled distribution alignment.

Discrete Distribution Estimation (DDE)

Conventional SSR methods typically predict the score by directly mapping the input sample x_i to the target value y . However, this approach is highly sensitive to noise and irrelevant features, often resulting in poor generalization and a high risk of overfitting, especially when few labels are available. Therefore, inspired by (Gao et al. 2017; Xu, Liu, and Geng 2019), we define several buckets $\mathcal{B} = \{\mathbf{b}_i\}_{i=1}^L$ based on the range of ground truth y , converting the regression task into a discrete distribution estimation problem. The obtaining of \mathcal{B} and the size L depend on the y , if we assume the bucket capacity is c , $\mathbf{b}_i = (i-1) \times c$, where each score is assigned to one corresponding bucket. Then, y can be obtained by calculating the expectation as follows:

$$y = \sum_{i=1}^L \tilde{p}_i \mathbf{b}_i \quad (1)$$

where \tilde{p}_i is the output probability of the model with the corresponding bucket \mathbf{b}_i . Therefore, the mapping function f in SSR is modified to learn a distribution $\mathcal{P} = \{p_i\}_{i=1}^L$ over predefined buckets. By transforming the numerical regression into an interval prediction problem, DDE offers a smoother learning objective and richer label distribution than direct numerical regression, leading to more effective use of limited labels and better noise robustness.

To obtain a probabilistic distribution, we apply the softmax function, and the predicted distribution is formulated as:

$$p_i = \frac{\exp(\tilde{p}_i)}{\sum_{i=1}^L \exp(\tilde{p}_i)} \quad (2)$$

where p_i is the predicted probability for the bucket \mathbf{b}_i after softmax. These outputs form a distribution, from which we compute the expectation to obtain the final score as follows:

$$\hat{y}_i = \sum_{i=1}^L p_i \mathbf{b}_i \quad (3)$$

Finally, we employ the MAE loss to minimize the distance between the prediction \hat{y}_i and the ground truth y_i :

$$\mathcal{L} = \frac{1}{|\mathcal{X}|} \sum_{x_i \in \mathcal{X}} |y_i - \hat{y}_i| \quad (4)$$

where y_i and the \hat{y}_i are the ground truth label and the predicted score of sample x_i , respectively. $|\mathcal{X}|$ is the number of samples in \mathcal{X} . In DRILL, both the teacher and student models utilize the MAE loss function to incorporate supervised information, as detailed below.

Distillation for Semi-supervised Regression

Since using DDE alone is insufficient for effective representation learning, we reformulate the knowledge distillation

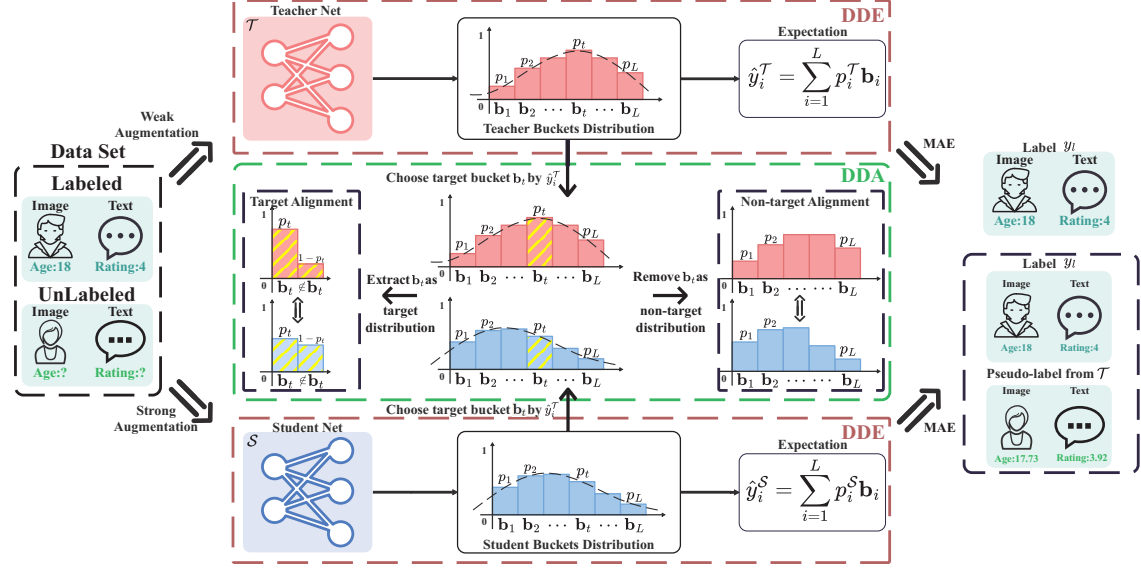


Figure 2: The Overview of DRILL. (1) The input includes both labeled and unlabeled data, and the weak and strong augmentations are applied to the teacher and student models, respectively. The teacher model is exclusively trained on the labeled data and is then used to generate pseudo labels for the unlabeled samples. The student model is trained on the entire dataset, utilizing the ground-truth labels for labeled samples and the pseudo labels for the unlabeled ones. (2) The DDE transforms score prediction into a classification task over discrete buckets, effectively mitigating the risk of overfitting. (3) The DDA first identifies the target bucket to construct a binary probability distribution, then aligns the predicted distributions over buckets between the teacher and student models separately for the target and non-target parts. This decoupled alignment enables the student model to focus on critical information and learn more generalized representations.

process to enable the student model to learn more generalized features for improved performance in SSR. To build the distillation framework for SSR, we first apply weak augmentation to the data before feeding it into the teacher model, while strong augmentation is applied to the input of the student model. The predicted scores from the teacher model are used to guide the student by assigning corresponding pseudo-labels to the unlabeled nodes. As a result, the student model is trained on the entire dataset, including both labeled samples and unlabeled samples with pseudo-labels. The loss functions for the teacher and student models are thus defined separately as follows.

$$\mathcal{L}_T = \frac{1}{|\mathcal{X}_l|} \sum_{x_i \in \mathcal{X}_l} |y_i - \hat{y}_i^T| \quad (5)$$

$$\mathcal{L}_S = \frac{1}{|\mathcal{X}|} \sum_{x_i \in \mathcal{X}} |y_i - \hat{y}_i^S| \quad (6)$$

where \hat{y}_i^T and \hat{y}_i^S are the predicted scores of the teacher model and the student model, respectively. To enable the student model to learn more accurate information for SSR, we define the loss \mathcal{L}_{DRILL} as follows, based on the joint training of the teacher and student models.

$$\mathcal{L}_{DRILL} = \mathcal{L}_T + \mathcal{L}_S + \mathcal{L}_{Alignment} \quad (7)$$

The joint training mechanism enables the teacher model to generate high-quality pseudo labels from a small amount

of labeled data, continuously improving the utilization of unlabeled data. The alignment loss $\mathcal{L}_{Alignment}$ minimizes the distance between the representations of the student and teacher models, typically implemented using Kullback–Leibler (KL) divergence or Mean Squared Error Loss (MSE).

Decoupling Distribution Alignment (DDA)

Conventional alignment methods often use KL divergence or MSE to minimize the distance between the teacher and student models. However, these approaches may fail to capture fine-grained discrepancies, resulting in suboptimal knowledge transfer. To mitigate this issue, we propose a DDA strategy that aligns the distributions over the buckets at a more granular level, enabling the student model to capture informative and discriminative features. Besides, aligning the distribution of discretized prediction buckets is essential for effectively transferring knowledge from the teacher to the student. Furthermore, we empirically find that employing more advanced alignment strategies enables the student model to acquire richer and more effective knowledge, thereby enhancing the generalization ability of DRILL. Specifically, we first identify the target bucket to formulate a binary classification task, treating the remaining buckets as non-targets. The alignment is then performed separately on the target and non-target buckets.

Target bucket identification. Motivated by DKD (Zhao et al. 2022), which has proven effective in classification

tasks by minimizing the distance between representations of each class, we adopt a similar strategy to enhance knowledge transfer in the SSR. Since the entire dataset is fed into the teacher model, it is worth noting that the unlabeled samples do not provide supervision signals—only the labeled samples contribute to the MAE loss in the teacher model. But in the advanced alignment, we choose to involve the unlabeled samples to provide more consistent information. To be specific, to determine the target bucket, we use the ground-truth labels for the labeled samples and the pseudo-labels for the unlabeled ones.

Target and non-target bucket distribution alignment. Based on the identification of the target bucket, we can split the bucket into the target distribution to formulate the $\mathbf{p} = \{p_t, 1 - p_t\}$, with \mathbf{p}^T and \mathbf{p}^S to represent the teacher and student. The results of buckets refer to the non-target distribution, denoted as $\mathbf{q} = \{p_1, p_2, \dots, p_L\}/p_t$, with \mathbf{q}^T and \mathbf{q}^S to represent the teacher and student. The optimization of DDA can be reformulated as the following:

$$\mathcal{L}_{DDA} = \text{KL}(\mathbf{p}^T, \mathbf{p}^S) + \beta \times \text{KL}(\mathbf{q}^T, \mathbf{q}^S) \times R \quad (8)$$

where $\text{KL}(\mathbf{p}^T, \mathbf{p}^S)$ aims to measure the similarity between the teacher distribution and student distribution on the target bucket. $\text{KL}(\mathbf{q}^T, \mathbf{q}^S)$ is the similarity on the non-target bucket. But we developed a conditional similarity based on the prediction variance σ^T by multiplying the factor $R = \max(1 - \sigma^T, 0)$ instead of using the original one. β is the hyperparameter to control the weight of non-target bucket distribution alignment. By minimizing the similarity of the target distribution and non-target distribution, DDA transfers the general distribution alignment into the binary classification task on the target bucket, while the alignment of the non-target bucket can effectively capture fine-grained information, serving as complementary information. The together use of the two component significantly enhances the student model’s ability to acquire more generalized knowledge across different domains.

Training and Inference

Training. During training, the DRILL adopts the proposed distillation framework by jointly training the teacher and student model with corresponding MAE loss functions \mathcal{L}_T and \mathcal{L}_S . The $\mathcal{L}_{Alignment}$ is implemented by the \mathcal{L}_{DDA} , which is formulated as the following:

$$\mathcal{L}_{DRILL} = \mathcal{L}_T + \mathcal{L}_S + \mathcal{L}_{DDA} \quad (9)$$

Inference. During inference, we solely use the student model to predict the score of a sample x_i in the test set \mathcal{X}_{Test} , as the student model is expected to learn rich and generalized knowledge from the teacher by leveraging the DDA. Give the unlabeled sample x_i in the \mathcal{X}_{Test} , the predicted score for the unlabeled sample, denoted as \hat{y}_i :

$$\hat{y}_i = \sum_{i=1}^L p_i^S \mathbf{b}_i \quad (10)$$

where p_i^S is the prediction of the student model and \mathbf{b}_i is the value of the bucket.

Experiments

Datasets. We conduct experiments on four real-world regression benchmark datasets spanning computer vision, speech, natural language processing, and clinical data analysis: (1) BVCC (Cooper and Yamagishi 2021) is an audio dataset that is utilized for predicting the perceptual quality of audio samples. (2) Yelp (Asghar 2016) is a dataset consisting of text that assesses the rating of customers. It is used for sentiment intensity regression. (3) UTKFace (Zhang, Song, and Qi 2017) is an image dataset used for estimating age from facial images. (4) MIMIC (Johnson et al. 2023) is a medical tabular dataset that is used for predicting the Sequential Organ Failure Assessment (SOFA) score. Table 1 summarizes their key statistics. More details about datasets are available in APP. A of our supplementary materials.

Model	BVCC	Yelp	UTKFace	MIMIC
# Train Set	4,974	250,000	18,964	3,623,503
# Test Set	1,066	25,000	4,741	55,859
Domain	Audio	Text	Image	Medical

Table 1: The statistical information of four datasets from four different domains.

Competing Methods. The competing methods can be categorized into three groups: direct regression, pseudo-label generation, and surrogate task-based approaches. (1) We directly predict the score by optimizing it using the MAE loss function, referred to as Direct Regression (DR). (2) The pseudo-label generation-based methods typically leverage the consistency regularization methods, including five technical approaches: perturbation-based self-ensembling frameworks, including π -model (Laine and Aila 2017); momentum-averaged teacher mechanisms with exponentially moving average, such as mean teacher (Tarpainen and Valpoli 2017); instance-level contrastive learning methods, exemplified by CLSS (Dai et al. 2023); co-training architectures like the dual-branch framework UCVME (Dai et al. 2023); entropy-regularized constraint approaches typified by MixMatch (Berthelot et al. 2019); (3) The surrogate task-based approach is RankUp (Huang, Fu, and Tsao 2024), which improves SSR with an auxiliary ranking classifier. More details can be found in App. B.

Evaluation Metric. Following the previous work (Huang, Fu, and Tsao 2024; Dai et al. 2023), we adopt three widely-used metrics to quantitatively assess the performance of DRILL and other competing methods, including Mean Absolute Error (MAE), the Coefficient of Determination (R^2), and the Spearman Rank Correlation Coefficient (SRCC). MAE quantifies the average absolute deviation between the model’s predictions and the true values. Lower MAE indicates better predictive accuracy. The SRCC quantifies the monotonic relationship between the predicted and ground-truth rankings, reflecting the proportion of variance in the target variable captured by the model. See the detailed description of each evaluation metric in the App. B.

Implementation Details. Our DRILL model is implemented in Python 3.10 with PyTorch 2.1.2. All experi-

Model	BVCC			Yelp			UTKFace			MIMIC		
	MAE ↓	R^2 ↑	SRCC ↑	MAE ↓	R^2 ↑	SRCC ↑	MAE ↓	R^2 ↑	SRCC ↑	MAE ↓	R^2 ↑	SRCC ↑
DR	0.533	0.490	0.741	0.723	0.566	0.769	9.420	0.540	0.712	2.726	0.239	0.510
π -Model (2017)	0.534	0.489	0.740	0.730	0.565	0.769	9.450	0.534	0.706	2.725	0.240	0.506
Mean Teacher (2017)	0.532	0.492	0.742	0.730	0.565	0.769	8.850	0.586	0.745	2.724	0.240	0.507
MixMatch (2019)	0.597	0.353	0.626	0.886	0.381	0.660	7.950	0.692	0.832	2.707	0.252	0.514
CLSS (2023)	0.499	0.534	0.748	0.721	0.543	0.748	9.100	0.586	0.737	2.714	0.251	0.510
UCVME (2023)	0.498	0.553	0.774	0.775	0.540	0.763	8.630	0.626	0.767	<u>2.656</u>	<u>0.285</u>	<u>0.539</u>
RankUp (2024)	<u>0.470</u>	<u>0.588</u>	<u>0.776</u>	<u>0.661</u>	<u>0.645</u>	<u>0.829</u>	<u>7.060</u>	<u>0.751</u>	<u>0.835</u>	2.720	0.244	0.509
DRILL (Ours)	0.422	0.669	0.818	0.549	0.694	0.839	6.852	0.761	0.838	2.629	0.291	0.541

Table 2: The comparison results on four datasets. The best performance is boldfaced, with the second-best underlined.

Model	BVCC			Yelp			UTKFace			MIMIC		
	MAE ↓	R^2 ↑	SRCC ↑	MAE ↓	R^2 ↑	SRCC ↑	MAE ↓	R^2 ↑	SRCC ↑	MAE ↓	R^2 ↑	SRCC ↑
SDE	<u>0.441</u>	<u>0.640</u>	<u>0.795</u>	0.717	0.514	0.728	9.570	0.505	0.687	2.748	0.227	0.481
DRILL-Logits	0.506	0.529	0.737	<u>0.576</u>	<u>0.655</u>	<u>0.819</u>	7.981	0.648	0.799	2.707	0.248	0.520
DRILL-KL	0.500	0.547	0.747	0.610	0.617	0.8033	<u>7.502</u>	<u>0.693</u>	<u>0.808</u>	<u>2.674</u>	<u>0.264</u>	<u>0.531</u>
DRILL (Ours)	0.422	0.669	0.818	0.549	0.694	0.839	6.852	0.761	0.838	2.629	0.291	0.541

Table 3: Ablation studies on the proposed model. The best performance is highlighted in bold, with the second-best underlined.

ments are conducted on a GeForce RTX 1080 GPU with 12 GB memory. The experimental configurations for DRILL strictly adhere to those described in (Huang, Fu, and Tsao 2024). In this paper, we set $\beta = 10$ for all of the datasets. The number of buckets L is set to 200 by default for the BVCC, Yelp, and UTKFace datasets, and 100 for the MIMIC dataset. To ensure fair comparison across methods, we adopt the same augmentation schemes in RankUp (Huang, Fu, and Tsao 2024). We apply weak augmentation to enrich the teacher’s knowledge, while strong augmentation is applied to the student to enhance generalization. More detailed parameter configurations and data augmentation mechanisms are provided in the App. C.

Main Comparison Results

Table 2 summarizes the performance of various methods across four datasets from four domains. All semi-supervised methods were trained on 250 labeled samples and evaluated on the test set. From the results, we observe that DRILL significantly outperforms tested semi-supervised regression methods across all datasets. Specifically, DRILL achieves yields significant improvements: at least a 16.9% reduction in MAE on Yelp, and a 13.8% increase in R^2 along with a 5.4% increase in SRCC on BVCC. Although RankUp achieved second-best performance across multiple datasets, it consistently underperformed DRILL on all tested benchmarks. This indicates that its sample ranking consistency-based strategy fails to fully leverage pseudo-label information and that its binary ranking classifier is more prone to overfitting. Conversely, DRILL achieves SOTA performance by leveraging more fine-grained label distribution information to reveal their ordinal and interval relationships, while mitigating model overfitting through DDE.

The consistency regularization-based methods like the π -model, Mean Teacher, and MixMatch, which apply a consistency loss based on various data augmentations, consistently

exhibit inferior performance across most datasets, merely matching the efficacy of DP on most datasets. The main reason is that their hybrid augmentation struggles to generate high-quality numeric pseudo-labels for the regression task, particularly under extremely limited sample conditions. In contrast, DRILL leverages DDE to transform continuous pseudo-labels into more explicit discrete buckets, thereby not only enhancing pseudo-label generation quality but also more effectively utilizing inter-label information, which collectively improves its suitability for SSR tasks.

As for the co-trained method, UCVME, which maximizes variational mutual information, yields suboptimal results on the MIMIC dataset. However, it requires a more complex Bayesian neural network to perform uncertainty variational inference for refining numeric pseudo-labels. In contrast, DRILL directly converts the regression problem into a discrete bucket estimation and leverages DDA to further enhance pseudo-labels, consequently surpassing UCVME in both accuracy and efficiency. Moreover, DRILL also consistently outperforms CLSS due to its superior capability in learning more generalized feature representations.

Ablation Study

In this section, we perform an ablation study to evaluate the contribution of each component in DRILL. We design three variants, including (1) Single-DDE (**SDE**), we remove the distillation framework, only keep the one branch, and train the DDE on the labeled samples. This is to evaluate the effectiveness of the proposed distillation framework. (2) **DRILL-Logits**, which replace DDA with the logit distill *i.e.*, label alignment. (3) **DRILL-KL**, which replaces the DDA with KL divergence. Both DRILL-KL and DRILL-Logits are used to evaluate the effectiveness of DDA. The results are shown in Table 3. From the results, the DRILL can consistently outperform all the variants and yields the best performance on all the datasets, demonstrating its ef-

fectiveness. Both DRILL-KL and DRILL-Logits underperform the full DRILL model but outperform SDE on the Yelp, UTKFace, and MIMIC datasets. This demonstrates that distillation effectively captures generalized patterns across text, image, and tabular medical data modalities. On the BCCV dataset, SDE achieves the second-best performance, though still behind DRILL. This suggests that while SDE, leveraging only DDE, can effectively learn patterns in audio data, the absence of distillation and DDA limits its ability to capture fine-grained information, leading to suboptimal results.

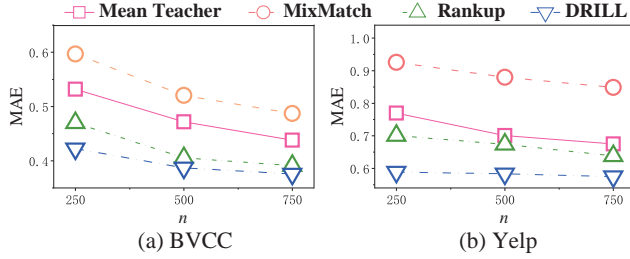


Figure 3: The MAE values w.r.t of labeled sample size n .

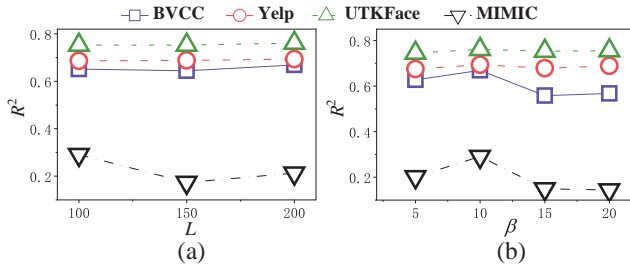


Figure 4: The effectiveness of hyperparameters.

Performance w.r.t. Labeled Sample Size

To explore the impact of labeled samples, we compare DRILL with the competing methods, using varying numbers of labeled samples, with the results reported in Fig. 3. As the number of labeled samples increases, DRILL generally improves across the datasets, which is consistent with other semi-supervised methods. Under different label rates, our DRILL consistently maintains the best performance with the lowest MAE, showing the superiority of our method.

Sensitive Analysis

We evaluate the sensitivity of DRILL w.r.t. the hyperparameter bucket size L and β in \mathcal{L}_{DDA} . The results are shown in Fig. 4. The results on more datasets can be found in App.D.

Performance w.r.t. Hyperparameter L : As shown in the Fig. 4(a), DRILL performs stably under different buckets on text, image, and audio datasets, and the performance slightly improves as L increases. The main reason lies in the capacity of larger buckets to capture the intricate relationships within the label distribution more accurately. In contrast, on the MIMIC dataset, DRILL achieved its highest performance with 100 buckets, primarily because SOFA scores

Model	MIMIC	Yelp	UTKFace	BVCC
UCVME (2023)	19	108	30	112
RankUp (2024)	10	28	43	46
DRILL (ours)	15	34	150	66

Table 4: Runtimes (in seconds) on the four datasets on GPU.

are more concentrated within a specific interval (typically around 4-10 in certain cohorts) compared to other datasets, and smaller buckets are already capable of capturing sufficient label distribution information.

Performance w.r.t. Hyperparameter β in \mathcal{L}_{DDA} : As shown in the Fig. 4(b), DRILL exhibited a consistent trend across all tested datasets, achieving optimal performance when beta was set to 10. The main reason is that a smaller β might cause the model to emphasize the ‘difficulty’ of training samples, while a larger β forces it to learn more generalized non-target information from the Student network. An effective balance is achieved when beta is set to 10.

Efficiency Analysis

Time Complexity In this section, we analyze the time complexity of DRILL. Given that both models share the same backbone output as input, the computational cost of the backbone is excluded from this analysis. (1) The DDE module comprises a fully connected layer and an expectation computation. Its time complexity is $\mathcal{O}(LM + 2L)$, where M denotes the dimension of the backbone output feature and L represents the number of buckets. (2) The DDA module consists of two components: distribution distillation and regression distillation. Their respective time complexities are $\mathcal{O}(L)$ and $\mathcal{O}(1)$ per sample. Consequently, the overall time complexity of DRILL is $\mathcal{O}(2LM + 5L)$.

Running Time Analysis. The runtimes of DRILL and two recently proposed semi-supervised methods—including both training and inference time—on GPU are reported in Table 4. DRILL generally demonstrates higher efficiency on tabular medical data, text, and audio datasets. Although it requires more time on image datasets, this overhead is acceptable given the performance gains. Overall, DRILL offers a favorable trade-off between efficiency and effectiveness.

Conclusion and Future Work

In this paper, we propose DRILL, the very first decouple representation distillation framework for semi-supervised regression. DRILL is implemented by the DDE, where we transform the score prediction task into the discrete buckets distribution estimation to mitigate the risk of overfitting. Then, the DDA is proposed to enhance the generalization by aligning the target buckets and non-target buckets between the teacher and student on the distribution of buckets. Extensive experimental results across multiple datasets spanning four domains—audio, image, text, and tabular medical data—demonstrate that DRILL outperforms state-of-the-art methods, indicating its superior generalization capability. Exploring more data modalities and developing a unified semi-supervised regression framework are left as directions for future work.

References

Asghar, N. 2016. Yelp dataset challenge: Review rating prediction. *arXiv preprint arXiv:1605.05362*.

Berthelot, D.; Carlini, N.; Goodfellow, I.; Papernot, N.; Oliver, A.; and Raffel, C. A. 2019. Mixmatch: A holistic approach to semi-supervised learning. *Advances in neural information processing systems*, 32.

Chen, L.; Wang, D.; Gan, Z.; Liu, J.; Henao, R.; and Carin, L. 2021. Wasserstein contrastive representation distillation. In *Proceedings of the IEEE/CVF conference on computer vision and pattern recognition*, 16296–16305.

Cooper, E.; and Yamagishi, J. 2021. How do Voices from Past Speech Synthesis Challenges Compare Today? In *11th ISCA Speech Synthesis Workshop (SSW 11)*, 183–188. ISCA.

Cubuk, E. D.; Zoph, B.; Shlens, J.; and Le, Q. V. 2020. Randaugment: Practical automated data augmentation with a reduced search space. In *Proceedings of the IEEE/CVF conference on computer vision and pattern recognition workshops*, 702–703.

Dai, W.; Du, Y.; Bai, H.; Cheng, K.-T.; and Li, X. 2023. Semi-supervised contrastive learning for deep regression with ordinal rankings from spectral seriation. *Advances in Neural Information Processing Systems*, 36: 57087–57098.

Dai, W.; Li, X.; and Cheng, K.-T. 2023. Semi-supervised deep regression with uncertainty consistency and variational model ensembling via bayesian neural networks. In *Proceedings of the AAAI Conference on Artificial Intelligence*, volume 37, 7304–7313.

Feng, S.; Zhang, H.; Xi, B.; Zhao, C.; Li, Y.; and Chanussot, J. 2024. Cross-domain few-shot learning based on decoupled knowledge distillation for hyperspectral image classification. *IEEE Transactions on Geoscience and Remote Sensing*.

Gao, B.-B.; Xing, C.; Xie, C.-W.; Wu, J.; and Geng, X. 2017. Deep label distribution learning with label ambiguity. *IEEE Transactions on Image Processing*, 26(6): 2825–2838.

Gou, J.; Yu, B.; Maybank, S. J.; and Tao, D. 2021. Knowledge distillation: A survey. *International journal of computer vision*, 129(6): 1789–1819.

Gui, J.; Chen, T.; Zhang, J.; Cao, Q.; Sun, Z.; Luo, H.; and Tao, D. 2024. A survey on self-supervised learning: Algorithms, applications, and future trends. *IEEE Transactions on Pattern Analysis and Machine Intelligence*, 46(12): 9052–9071.

Hinton, G.; Vinyals, O.; and Dean, J. 2015. Distilling the knowledge in a neural network. *arXiv preprint arXiv:1503.02531*.

Huang, P.-Y.; Fu, S.-W.; and Tsao, Y. 2024. RankUp: Boosting semi-supervised regression with an auxiliary ranking classifier. *Advances in Neural Information Processing Systems*, 37: 107444–107468.

Huang, T.; Zhang, Y.; Zheng, M.; You, S.; Wang, F.; Qian, C.; and Xu, C. 2023. Knowledge diffusion for distillation. *Advances in Neural Information Processing Systems*, 36: 65299–65316.

Jean, N.; Xie, S. M.; and Ermon, S. 2018. Semi-supervised deep kernel learning: Regression with unlabeled data by minimizing predictive variance. *Advances in Neural Information Processing Systems*, 31.

Jin, Y.; Wang, J.; and Lin, D. 2023. Multi-level logit distillation. In *Proceedings of the IEEE/CVF Conference on Computer Vision and Pattern Recognition*, 24276–24285.

Jo, Y.; Kahng, H.; and Kim, S. B. 2024. Deep semi-supervised regression via pseudo-label filtering and calibration. *Applied Soft Computing*, 161: 111670.

Johnson, A. E.; Bulgarelli, L.; Shen, L.; Gayles, A.; Shamout, A.; Horng, S.; Pollard, T. J.; Hao, S.; Moody, B.; Gow, B.; et al. 2023. MIMIC-IV, a freely accessible electronic health record dataset. *Scientific data*, 10(1): 1.

Laine, S.; and Aila, T. 2017. Temporal Ensembling for Semi-Supervised Learning. In *International Conference on Learning Representations*.

Lee, D.-H.; et al. 2013. Pseudo-label: The simple and efficient semi-supervised learning method for deep neural networks. In *Workshop on challenges in representation learning, ICML*, volume 3, 896. Atlanta.

Li, Y.; Wang, Y.; and Cui, Z. 2023. Decoupled multi-modal distilling for emotion recognition. In *Proceedings of the IEEE/CVF conference on computer vision and pattern recognition*, 6631–6640.

Li, Z.; Li, X.; Yang, L.; Zhao, B.; Song, R.; Luo, L.; Li, J.; and Yang, J. 2023. Curriculum temperature for knowledge distillation. In *Proceedings of the AAAI Conference on Artificial Intelligence*, volume 37, 1504–1512.

Mey, A.; and Loog, M. 2023. Improved Generalization in Semi-Supervised Learning: A Survey of Theoretical Results. *IEEE Transactions on Pattern Analysis and Machine Intelligence*, 45(4): 4747–4767.

Min, Z.; Bai, J.; and Li, C. 2024. Leveraging local variance for pseudo-label selection in semi-supervised learning. In *Proceedings of the AAAI Conference on Artificial Intelligence*, volume 38, 14370–14378.

Mohammadi Foumani, N.; Miller, L.; Tan, C. W.; Webb, G. I.; Forestier, G.; and Salehi, M. 2024. Deep learning for time series classification and extrinsic regression: A current survey. *ACM Computing Surveys*, 56(9): 1–45.

Qiao, H.; Chen, L.; and Zhu, F. 2022. Ranking convolutional neural network for Alzheimer’s disease mini-mental state examination prediction at multiple time-points. *Computer Methods and Programs in Biomedicine*, 213: 106503.

Sohn, K.; Berthelot, D.; Carlini, N.; Zhang, Z.; Zhang, H.; Raffel, C. A.; Cubuk, E. D.; Kurakin, A.; and Li, C.-L. 2020. Fixmatch: Simplifying semi-supervised learning with consistency and confidence. *Advances in neural information processing systems*, 33: 596–608.

Tarvainen, A.; and Valpola, H. 2017. Mean teachers are better role models: Weight-averaged consistency targets improve semi-supervised deep learning results. *Advances in neural information processing systems*, 30.

Van Engelen, J. E.; and Hoos, H. H. 2020. A survey on semi-supervised learning. *Machine learning*, 109(2): 373–440.

Wang, Y.; Chen, H.; Fan, Y.; Sun, W.; Tao, R.; Hou, W.; Wang, R.; Yang, L.; Zhou, Z.; Guo, L.-Z.; et al. 2022. Usb: A unified semi-supervised learning benchmark for classification. *Advances in Neural Information Processing Systems*, 35: 3938–3961.

Xie, Q.; Dai, Z.; Hovy, E.; Luong, T.; and Le, Q. 2020a. Unsupervised data augmentation for consistency training. *Advances in neural information processing systems*, 33: 6256–6268.

Xie, Q.; Luong, M.-T.; Hovy, E.; and Le, Q. V. 2020b. Self-training with noisy student improves imagenet classification. In *Proceedings of the IEEE/CVF conference on computer vision and pattern recognition*, 10687–10698.

Xu, N.; Liu, Y.-P.; and Geng, X. 2019. Label enhancement for label distribution learning. *IEEE Transactions on Knowledge and Data Engineering*, 33(4): 1632–1643.

Yang, X.; Song, Z.; King, I.; and Xu, Z. 2022. A survey on deep semi-supervised learning. *IEEE transactions on knowledge and data engineering*, 35(9): 8934–8954.

Yang, Y.; Jiang, N.; Xu, Y.; and Zhan, D.-C. 2024. Robust semi-supervised learning by wisely leveraging open-set data. *IEEE Transactions on Pattern Analysis and Machine Intelligence*, 46(12): 8334–8347.

Zhang, T.; Luo, Y.; Wang, X.; and Kwong, S. 2025. Semi-supervised segmentation on medical images with pseudo label calibration and neural process. *Neural Networks*, 107510.

Zhang, Z.; Song, Y.; and Qi, H. 2017. Age progression/regression by conditional adversarial autoencoder. In *Proceedings of the IEEE conference on computer vision and pattern recognition*, 5810–5818.

Zhao, B.; Cui, Q.; Song, R.; Qiu, Y.; and Liang, J. 2022. Decoupled knowledge distillation. In *Proceedings of the IEEE/CVF Conference on computer vision and pattern recognition*, 11953–11962.

Zheng, N.; Song, X.; Dong, X.; Ghosh, A. N.; Nie, L.; and Zimmermann, R. 2025. Language-Assisted Debiasing and Smoothing for Foundation Model-Based Semi-Supervised Learning. In *Proceedings of the Computer Vision and Pattern Recognition Conference*, 25708–25717.

Appendix

A. Datasets

A detailed introduction of all the datasets used in our work is given as follows.

BVCC (Cooper and Yamagishi 2021) serves as an audio quality assessment benchmark, where the objective is to predict the perceptual quality of audio samples. Annotated on a 1-to-5 scale, the labels represent averaged scores from multiple listeners. This dataset comprises 4,974 training samples, 1,066 validation samples, and 1,066 test samples. Following the protocol defined in Rankup (Huang, Fu, and Tsao 2024), we exclusively utilize the training and validation splits for performance evaluation.

Yelp (Asghar 2016) focuses on textual opinion mining, targeting the prediction of customer ratings based on reviews posted on the Yelp platform. The five-class rating labels represent distinct satisfaction levels. We employ the preprocessed Yelp data provided in the USB codebase (Huang, Fu, and Tsao 2024), consisting of 250,000 training samples, 25,000 validation samples, and 10,000 test samples. Consistent with RankUp’s methodology, only the training split is used for model training, while evaluation is performed on the validation set.

UTKFace (Zhang, Song, and Qi 2017) addresses image-based age estimation, aiming to predict the age of individuals depicted in facial images. The age labels range from 1 to 116 years. RankUp partitions this dataset into 18,964 training samples and 4,741 test samples, with experiments conducted on its aligned and cropped version.

MIMIC (Johnson et al. 2023) presents a multivariate time-series score prediction task, where the objective is to forecast SOFA scores (indicating illness severity from 0 to 24) based on patients’ clinical features over time. This dataset contains 3,623,503 training samples and 55,859 test samples.

B. Competing Methods

A more detailed introduction of the six competing models and the evaluation metrics adopted in our work is given as follows.

B1. Description of Baselines

π -Model (Laine and Aila 2017) achieves self-ensembling by aggregating the outputs of a single network at different training stages. Consensus predictions for unknown labels are formed through diverse regularization and augmentation strategies. Perturbations are injected into both branches, and consistency between the two perturbed outputs is enforced, ensuring a more balanced and symmetric comparison.

Mean Teacher (Tarvainen and Valpola 2017) aims to train a model via consistency between original samples and their perturbed counterparts, while using an exponential-moving-average (EMA) version of the model—termed the teacher—to supply more reliable guidance to the current student during training.

MixMatch (Berthelot et al. 2019) consolidates the dominant approaches in semi-supervised learning by generating

Models	Wide	Whisper	Bert	Bert
	ResNet-28-2	Base	Small	
Training Iterations	262,144	102,400	102,400	1024,000
Evaluation Iterations	1,024	1,024	1,024	1,024
Batch Size	32	8	8	8
Optimizer	SGD	AdamW	AdamW	AdamW
Momentum	0.9	-	-	-
Criterion	MAE	MAE	MAE	MAE
Weight Decay	1e-03	2e-05	5e-04	2e-5
Layer Decay	1.0	0.75	0.75	0.75
Learning Rate	1e-02	2e-06	1e-05	2e-06
EMA Weight	0.999	-	-	0.999
Pretrained	False	True	True	False
Sampler	Random	Random	Random	Random
Image Resize	40x40	-	-	-
Max Length Seconds	-	6.0	-	-
Sample Rate	-	16,000	-	-
Max Length	-	-	512	-

Table 5: The default hyperparameters for the base models.

low-entropy label guesses for augmented unlabeled examples and subsequently blending labeled and unlabeled data via MixUp.

CLSS (Dai et al. 2023) extends contrastive regression to the semi-supervised domain. It exploits a spectral ordering algorithm to extract ordinal rankings from the feature-similarity matrix of unlabeled data and then leverages these rankings as supervisory signals. The additional ranking loss enhances robustness, marking the first exploration of contrastive learning for regression tasks.

UCVME (Dai, Li, and Cheng 2023) improves training by producing high-quality uncertainty estimates for pseudo-labels via heteroscedastic regression. By explicitly modeling label uncertainty, the approach assigns greater importance to more reliable pseudo-labels. Furthermore, a novel variational model-ensembling scheme is introduced to reduce predictive noise and generate stronger pseudo-labels.

RankUp (Huang, Fu, and Tsao 2024) reframes the original regression task as a ranking problem and trains it jointly with the regression objective. By introducing an auxiliary ranking classifier whose outputs can be handled by any off-the-shelf semi-supervised classification method, RankUp seamlessly integrates existing classification techniques into regression-oriented semi-supervised learning.

B2. Evaluation Metric

We used Mean Absolute Error (MAE), R^2 , and Spearman’s Rank Correlation Coefficient (SRCC) as evaluation metrics for the tested model. The calculation process for each metric is as follows:

MAE: measures the average magnitude of the errors in a set

Models	II-Model, MeanTeacher	MixMatch	UCVME	CLSS	RankUp	DRILL
Unlabeled Batch Ratio	1.0	1.0	1.0	0.25	7.0	7.0
Regression Unlabeled Loss Ratio	0.1	0.1	0.05	-	-	-
Regression Unlabeled Loss Warmup	0.4	0.4	-	-	-	-
Mixup Alpha	-	0.5	-	-	-	-
Dropout Rate	-	-	0.05	-	-	-
Ensemble Number	-	-	5	-	-	-
CLSS Lambda	-	-	-	2.0	-	-
Labeled Contrastive Loss	-	-	-	1.0	-	-
Unlabeled Contrastive Loss	-	-	-	0.05	-	-
Unlabeled Rank Loss Ratio	-	-	-	0.01	-	-
ARC Unlabeled Loss Ratio	-	-	-	-	1.0	-
ARC Loss Ratio	-	-	-	-	0.2	-
Confidence Threshold	-	-	-	-	0.95	-
Temperature	-	-	-	-	0.5	-
β	-	-	-	-	-	10

Table 6: Specific hyperparameters for each semi-supervised regression method.

Dataset	Augmentation
UTKFace	Weak: Random Crop, Random Horizontal Flip Strong: RandAugment (Cubuk et al. 2020)
BVCC	Weak: Random Sub-sample Strong: Random Sub-sample, Mask, Trim, Padding
Yelp	Weak: None Strong: Back-Translation (Xie et al. 2020a)
MIMIC	Weak: Random Masking Strong: Operation Group

Table 7: Data augmentation strategies for different datasets.

of predictions, defined as follows:

$$\text{MAE} = \frac{1}{N} \sum_{i=1}^N |\hat{y}_i - y_i|,$$

where N denotes the number of samples, \hat{y}_i is the model’s prediction, and y_i is the corresponding ground-truth.

R^2 measures the proportion of variance in the ground-truth labels that is captured by the model. It is defined as

$$R^2 = 1 - \frac{\sum_{i=1}^N (\hat{y}_i - y_i)^2}{\sum_{i=1}^N (\bar{y} - y_i)^2},$$

where \bar{y} is the mean of the ground-truth labels. R^2 ranges from $(-\infty, 1]$; higher values indicate superior explanatory power. Let $r(\hat{y})$ and $r(y)$ denote the ranks of predictions and labels, respectively. Then

SRCC is a non-parametric measure of the statistical dependence between the rankings of two variables.

$$\text{SRCC} = \frac{\text{cov}(r(\hat{y}), r(y))}{\sigma_{r(\hat{y})} \sigma_{r(y)}},$$

with $\text{cov}(\cdot, \cdot)$ and σ denoting covariance and standard deviation, respectively. SRCC ranges from $[-1, 1]$, where the value closer to 1 implies a stronger rank-order.

C. Parameters and Data Augmentation

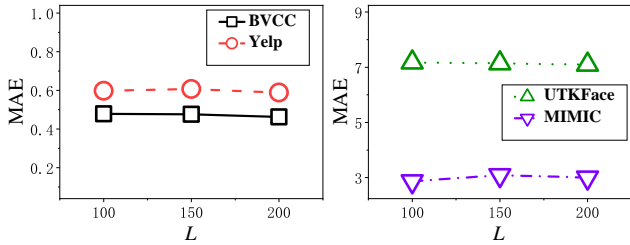
C1. Parameter Configurations of Base Models

In this work, we employ a distinct base model for each database: Whisper-Base for audio data on BVCC, Bert-Small for text data on Yelp, Wide ResNet-28-2 for image data on UTKFace, and BERT for time-series prediction of SOFA values on MIMIC medical data. The common parameter Configurations of all the base models as listed in Table 5. Specific hyperparameter configurations for each SSR method are provided in Table 6.

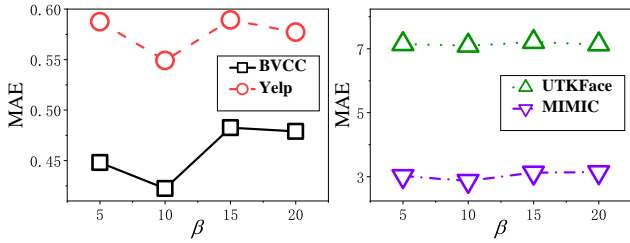
C2. Weak and Strong Augmentation

For audio, image, and text data, we adopt the universal semi-supervised learning benchmark framework, USB (Wang et al. 2022), to implement the weak and strong augmentations following the previous work (Huang, Fu, and Tsao 2024). For the MIMIC dataset, given its time-series nature, weak augmentation involves applying random masking operations, while strong augmentation employs m rounds of random masking combined with Gaussian noise injection for multivariate time-series data. Specifically, each random masking operation obscures 5% of the observed data. Each Gaussian noise application introduces additive noise sampled from a normal distribution with zero mean and a variance of 0.02. To ensure fair comparison across methods, the same augmentation strategy is applied to both DRILL and other comparative methods.

Detailed descriptions of data augmentation methods across different domains are presented in Table 7.



(a) The MAE w.r.t of bukets size L .



(b) The MAE w.r.t of β .

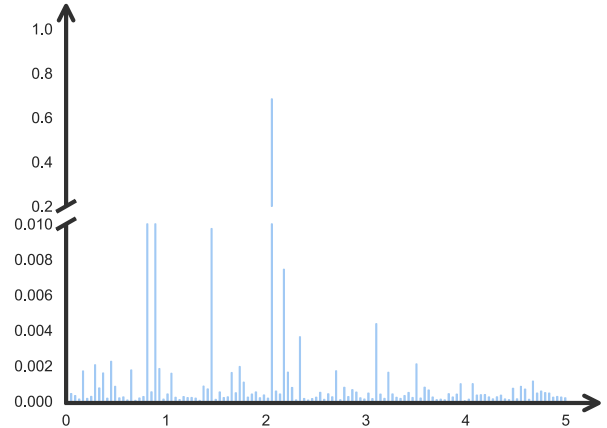
Figure 5: The effectiveness of the hyperparameters.

D. Additional Experimental Results

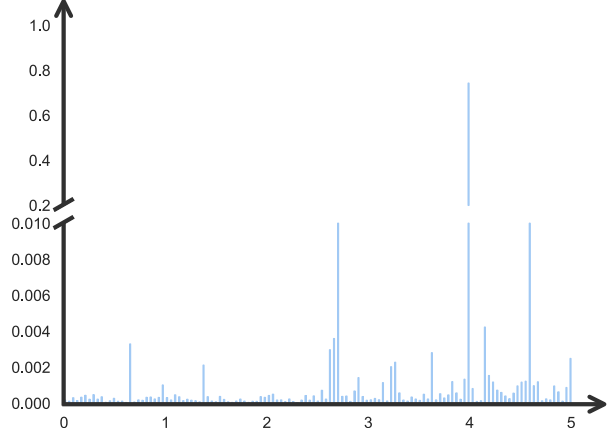
In this section, we further evaluate the effectiveness of the hyperparameters, specifically the bucket size of L and β , in \mathcal{L}_{DDA} using additional evaluation metrics. The results are shown in Fig.5. For the effectiveness of the bucket size L , compared to the R^2 metric, the MAE for DRILL exhibits greater stability under variations of L , see Fig.5 (a). We found that the best performance is achieved with 200 buckets for the BVCC, Yelp, and UTKFace datasets, while a lower MAE is obtained for the MIMIC dataset using 100 buckets. Regarding the effectiveness of β in \mathcal{L}_{DDA} , see Fig.5 (b), the MAE values demonstrate a trend comparable to that of R^2 across all datasets, with optimal performance universally observed at $\beta = 10$.

E. Visualization Results

Fig. 6 presents a visualization of the prediction cases using the DRILL model, illustrating the predicted discrete buckets and their associated probability values on the Yelp dataset. As shown in Fig. 6 (a), for a regression value of 2, the Yelp dataset score prediction is made using a distributed set of $L=200$ buckets that span the 0-to-5 rating range. Notably, in addition to the score of 2 (Fair/Dissatisfied) itself, the model primarily leverages the probabilities of the nearby related values of 1 (Poor/Very Dissatisfied) and 3 (Average/Neutral) for a combined prediction. A similar phenomenon can also be observed in the other example in Fig 6 (b). The results above demonstrate that DIRLL more effectively utilizes label distribution information, thereby improving SSR performance.



(a) DRILL model prediction example for a ground truth lable=2.



(b) DRILL model prediction example for a ground truth lable=4.

Figure 6: The visualization results of DRILL.